Kirk, T. K., & Shimada, M. (1985) in *Biosynthesis and Biodegradation of Wood Components* (Higuchi, T., Ed.) pp 579–605, Academic Press, New York.

Kirk, T. K., & Farrell, R. L. (1987) *Annu. Rev. Microbiol.* *41*, 465–505.

Kirk, T. K., Tien, M., Kersten, P. J., Mozuch, M. D., & Kalyanaraman, B. (1986) *Biochem. J. 236*, 279–287.

Kuila, D., Tien, M., Fee, J. A., & Ondrias, M. (1985) *Biochemistry 24*, 3394–3397.

Leisola, M. S. A., Schmidt, B., Thanei-Wyss, U., & Fiechter, A. (1985a) *FEBS Lett. 189*, 267–270.

Leisola, M. S. A., Thanei-Wyss, U., & Fiechter, A. (1985b) *J. Biotechnol. 3*, 97–107.

Leisola, M. S. A., Kozulic, B. Meussdoerffer, F., & Fiechter, A. (1987) *J. Biol. Chem. 262*, 419–424.

Miki, K., Renganathan, V., Mayfield, M. B., & Gold, M. H. (1987) *FEBS Lett. 210*, 199–203.

Palmer, J. M., Harvey, P. J., & Schoemaker, H. E. (1987) *Philos. Trans. R. Soc. London, A 321*, 495–502.

Rajagopalan, S., Seshadri, T. R., & Varadarajan, S. (1949) *Proc.—Indian Acad. Sci. 30A*, 265–270.

Renganathan, V., & Gold, M. H. (1986) *Biochemistry 25*, 1626–1631.

Renganathan, V., Miki, K., & Gold, M. H. (1985) *Arch. Biochem. Biophys. 241*, 304–314.

Renganathan, V., Miki, K., & Gold, M. H. (1986) *Arch. Biochem. Biophys. 246*, 155–161.

Russell, G. A. (1957) *J. Am. Chem. Soc. 79*, 3871–3877.

Schoemaker, H. E., Harvey, P. J., Bowen, R. M., & Palmer, J. M. (1985) *FEBS Lett. 183*, 7–12.

Shimada, M., Hattori, T., Umezawa, T., Higuchi, T., & Uzura, K. (1987) *FEBS Lett. 221*, 327–331.

Tien, M., & Kirk, T. K. (1983) *Science 221*, 661–663.

Tien, M., & Kirk, T. K. (1984) *Proc. Natl. Acad. Sci. U.S.A. 81*, 2280–2284.

Troller, J., Smit, J.-D., Leisola, M., Kallen, J., Winterhalter, K., & Fiechter, A. (1988) *Bio/Technology 6*, 571–573.

Umezawa, T., & Higuchi, T. (1986) *FEBS Lett. 205*, 293–298.

Umezawa, T., & Higuchi, T. (1987a) *FEBS Lett. 218*, 255–260.

Umezawa, T., & Higuchi, T. (1987b) *Agric. Biol. Chem. 51*, 2281–2284.

Umezawa, T., Shimada, M., Higuchi, T., & Kusai, K. (1986) *FEBS Lett. 205*, 287–292.

Walther, I., Kälin, M., Reiser, J., Suter, F., Fritsche, B., Saloheimo, M., Leisola, M. S. A., Teeri, T., Knowles, J., & Fiechter, A. (1988) *Gene* (in press).

Wanzlick, H. W., & Jahnke, U. (1968) *Chem. Res. 101*, 3744–3752.

Mechanism of GTP Hydrolysis in Tubulin Polymerization: Characterization of the Kinetic Intermediate Microtubule–GDP–P_i Using Phosphate Analogues

Marie-France Carlier,* Dominique Didry, Colette Simon, and Dominique Pantaloni

Laboratoire d'Enzymologie du CNRS, 91198 Gif-sur-Yvette, France

ABSTRACT: Beryllium fluoride (BeF_3^-) has previously been shown to bind tightly to microtubules as a structural analogue of P_i and to mimic the GDP–P_i transient state in tubulin polymerization [Carlier, M.-F., Didry, D., Melki, R., Chabre, M., & Pantaloni, D. (1988) *Biochemistry 27*, 3555–3559]. The interaction of BeF_3^- with tubulin is analyzed here in greater detail. BeF_3^- binds to and dissociates from microtubule GDP subunits at very slow rates ($k_+ \simeq 100$ M^{-1} s^{-1}; $k_- \simeq 6 \times 10^{-4}$ s^{-1}), suggesting that a slow conformation change of tubulin, linked to the stabilization of the microtubule structure, follows BeF_3^- binding. The possibility is evoked that BeF_3^- acts as a transition-state analogue in the GTPase reaction of tubulin. BeF_3^- does not bind to dimeric nor to oligomeric GDP–tubulin with high affinity. Substoichiometric binding of BeF_3^- to microtubules provides extensive stabilization of the structure. An original mechanistic model that accounts for the data is proposed. The kinetic parameters for microtubule elongation in the presence of GTP- and GDP–tubulin with and without BeF_3^- have been determined. Data support the following views: (i) Microtubules at steady state and in a regime of slow growth in the presence of GTP are stabilized by a cap of GDP–P_i subunits functionally similar to GDP–BeF_3 subunits. (ii) In the presence of BeF_3^-, microtubules elongate from GDP–tubulin within the following sequence of reactions: initial nonproductive binding of GDP–tubulin to microtubule ends is followed by the binding of BeF_3^- and the associated conformation change allowing sustained elongation.

The hydrolysis of tightly bound GTP that accompanies tubulin polymerization occurs on microtubules, following the incorporation of GTP subunits in the polymer (Weisenberg et al., 1976; Carlier & Pantaloni, 1981). GTP hydrolysis follows the elongation process closely when the rate of growth is slow, at low tubulin concentration and close to steady state; stretches of terminal GTP subunits develop at high tubulin concentration when the microtubule grows at a rate faster than the intrinsic rate of GTP hydrolysis (40 s^{-1}; Carlier et al., 1987a). In a regime of slow growth, terminal subunits dissociate from microtubules at a rate of 2 orders of magnitude slower than internal GDP subunits, therefore forming a stabilizing "cap" (Carlier, 1982; Hill & Carlier, 1983; Carlier et al., 1984a), initially thought to be a GTP cap. The pos-

sibility of loss of this cap, via statistic fluctuations of microtubule length, was hypothesized to be the basis for the "dynamic instability" of microtubules (Mitchison & Kirschner, 1984; Horio & Hotani, 1986). All these facts emphasize the view that GTP hydrolysis plays a regulatory role in microtubule assembly by modulating the strength of the tubulin–tubulin interactions in the polymer. In an effort of understand how the elementary reactions of GTP cleavage and P_i release are coupled to changes in the stability of the polymer, we have recently shown (Carlier et al., 1988a) that P_i as well as its structural analogues the fluoride complexes of aluminum and beryllium (Bigay et al., 1985) bind in a 1:1 ratio to GDP subunits in microtubules, presumably in the site of the γ-phosphate of GTP, and reconstitute a very stable GDP–P_i–microtubule from which GDP–P_i subunits dissociate extremely slowly as compared to GDP subunits. This result led to the following conclusions. (1) P_i release, and not cleavage of GTP, is the elementary step coupled to the destabilization of microtubule structure. (2) In a regime of slow growth and at steady state, the stabilizing cap that maintains the unstable GDP core is most likely made of GDP–P_i subunits. (3) Regulation of dynamic instability might be exerted via a modulation of the rate of liberation of P_i. Similar conclusions have been reached concerning ATP hydrolysis associated to actin polymerization [Carlier & Pantaloni, 1988; for a review see Korn et al. (1987)]. Experiments described in this paper have been designed with the aim to characterize in more detail the interaction of P_i analogues with tubulin and to understand the correlation between the stability of tubulin–tubulin interactions in microtubules and the nature of the nucleotide bound.

Materials and Methods

Chemicals. Morpholinoethanesulfonic acid (MES) was from Calbiochem. EGTA, diadenosine pentaphosphate, and hexokinase came from Sigma, beryllium sulfate (gold label) from Aldrich, and guanosine 5'-di- and triphosphate from Boehringer. [7]Be, [3H]GTP, and [γ-32P]GTP came from Amersham.

Tubulin. Tubulin was purified from pig brain by three cycles of polymerization (Shelanski et al., 1973) followed by phosphocellulose chromatography (Weingarten et al., 1975) and stored at −80 °C at a concentration of 40–80 μM in 50 mM MES, pH 6.8, 0.5 mM EGTA, 0.25 mM MgCl$_2$, 0.1 mM GTP, and 3.4 M glycerol (buffer A).

In all the experiments described here, polymerization buffer was buffer A supplemented with 6 mM MgCl$_2$ and containing GTP and/or GDP as indicated. Polymerization was monitored turbidimetrically at 350 nm.

The 1:1 3H-labeled GTP–tubulin complex was isolated free of unbound nucleotide by chromatography over Sephadex G-25 (PD-10, Pharmacia) following nucleotide exchange for 1 h at 0 °C, as described (Carlier et al., 1987a).

The 1:1 GDP–tubulin complex (60–80 μM) was prepared by resuspending in buffer A without GTP a pellet of microtubules that had been sedimented through a 30% sucrose cushion in buffer A containing no GTP and 6 mM MgCl$_2$. Following depolymerization at 0 °C, the resulting GDP–tubulin solution was clarified by centrifugation at 4 °C, 150000g for 30 min before use. Measurements of initial rate of microtubule growth and analysis of its dependence on the concentration of dimeric tubulin were carried out as described (Carlier et al., 1987a). The time course of microtubule depolymerization upon dilution was monitored by using the glass fiber filter assay initially described by Job et al. (1985) with some modification (Carlier et al., 1988a).
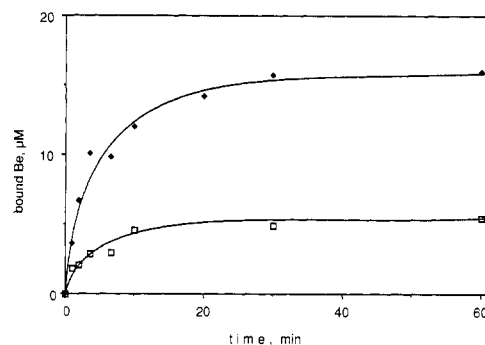

FIGURE 1: Time course of BeF_3^- binding to GDP subunits of microtubules. Tubulin was polymerized at 37 °C in buffer A containing 0.5 mM GTP. The concentration of polymerized subunits was 26 μM. At time zero, microtubules were reacted with 10 μM ($\square$) and 50 μM ($\blacklozenge$) 7Be-labeled Be^{2+} and 2 mM NaF. Aliquots were rapidly centrifuged in the airfuge at different time intervals following addition of BeF_3^-. The amount of BeF_3^- bound was determined as described under Materials and Methods. A delay of 30 s, necessary for the airfuge to reach maximum speed, was accounted for.

The kinetics of 7Be-labeled BeF$_3^-$ association to and dissociation from microtubules were monitored by using the sedimentation assay described (Carlier et al., 1988a). Microtubules were rapidly sedimented at 175000g for 5 min in the airfuge (Beckman) driven by a stream of heated air, at different times following either addition of 7Be-labeled BeF$_3$ to GDP–microtubules (association assay) or application of a chase of unlabeled Be to microtubules initially at equilibrium with a given amount of 7Be-labeled BeF$_3^-$ (dissociation assay). The amount of BeF$_3$ bound to microtubules was derived from the measurement of radioactive 7Be present in the supernatant, using a liquid scintillation spectrometer (Packard CA 2000).

Binding of BeF$_3^-$ to GDP–tubulin was investigated at 4 °C by the equilibrium dialysis technique using 7Be and altuglass cells containing 50 μL of solution in each compartment and equipped with Spectrapor 2 (Spectrum) dialysis membranes; 98% equilibrium of the ligand between the two compartments was reached within 3 h.

Histograms of microtubule length distribution were derived from electron micrographs of fixed and negatively stained samples as described (Carlier et al., 1987b).

Results

Kinetics of the Interaction between BeF$_3^-$ and Microtubules. Equilibrium binding studies have previously shown that BeF$_3^-$ binds tightly to GDP subunits of microtubules[1] (Carlier et al., 1988a). We now show that BeF$_3^-$ binds slowly to microtubules within the following second-order reaction:

$$BeF_3^- + (T\text{–}GDP)_{MT} \underset{k_-}{\overset{k_+}{\rightleftharpoons}} (T\text{–}GDP\text{–}BeF_3)_{MT}$$
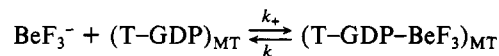
The time courses of association of 10 and 50 μM BeF$_3^-$ to 26 μM polymerized tubulin are displayed in Figure 1. The amount of BeF$_3$ bound at equilibrium was in good agreement with the value calculated by using an equilibrium dissociation constant $D_D = 12$ μM for binding of BeF$_3$ to microtubule

---

[1] The fact that binding of Be takes place in the presence of millimolar amounts of fluoride is a good indication that BeF$_3^-$, the predominant species in this range of F$^-$ concentration (Lange et al., 1986), is the actual ligand binding to GDP subunits of microtubules. However, since high-affinity binding of one particular beryllium fluoride complex to microtubules might displace the chemical equilibria existing in solution, a definite answer to the question of the structure of the bound beryllium fluoride species requires the actual measurement of the number of bound fluoride ions per Be atom in the site of the γ-phosphate of GTP.
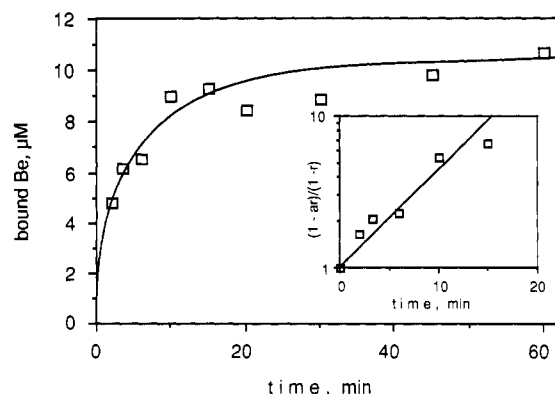
FIGURE 2: Second-order reaction of BeF_3^- with microtubules. Microtubules (24 μM polymerized subunits) were reacted with 24 μM ^{7}Be-labeled BeF_3 under the same conditions as in Figure 1. (Inset) Plot of the data according to eq 1.

Table I: Parameters for Interaction of Inorganic Phosphate and Its Analogues with Microtubules

	P_i	BeF_3^-
equilibrium dissociation constant K_D	25–35 mM	10–13 μM
association rate constant k_+	rapid equilibrium	90 $\pm$ 20 M^{-1} s^{-1}
dissociation rate constant k_-		6–10^{-4} s^{-1}

subunits (Carlier et al., 1988a). From the initial rates of reaction, a value of 95 $\pm$ 20 M^{-1} s^{-1} was derived for the association rate constant k_+. In addition, if BeF_3^- and microtubule subunits are reacted at identical concentrations, the overall time course of BeF_3 binding to microtubules can be described by the equation[2]

$$\log \frac{1 - ar}{1 - r} = \alpha t \tag{1}$$

where

$$r = \frac{(T-GDP-BeF_3(t))}{(T-GDP-BeF_3)_{eq}}$$

$$a = \left(\frac{(T-GDP-BeF_3^-)_{eq}}{(BeF_3^-)_0} \right)^2$$

$$\alpha = k_+ \frac{(BeF_3^-)_0^2 - (T-GDP-BeF_3)_{eq}^2}{(T-GDP-BeF_3)_{eq}}$$

Figure 2 shows the time course of binding of 24 μM BeF_3^- to 24 μM polymerized microtubule subunits and its analysis according to eq 1. A satisfactory fit to the overall time course was obtained with a k_+ value of 97 M^{-1} s^{-1}, in agreement with the preceding determination.

The kinetics of dissociation of BeF_3^- from the (T–GDP–BeF_3)$_{MT}$ complex was studied in a chase experiment as follows. Tubulin was polymerized at 46 μM and incubated with 10 μM ^{7}Be-labeled Be^{2+} and 2 mM NaF at 37 °C for 20 min, a time sufficient for the binding equilibrium to be reached. A chase of 100 μM unlabeled Be^{2+} was then applied to the sample, and aliquots were centrifuged at different time periods following the chase. The time course of displacement of unlabeled for labeled ligand was monitored by measuring the time-dependent increase in radioactive ^{7}Be in the supernatant of microtubules. Data, shown in Figure 3, indicate that BeF_3^- dissociates slowly
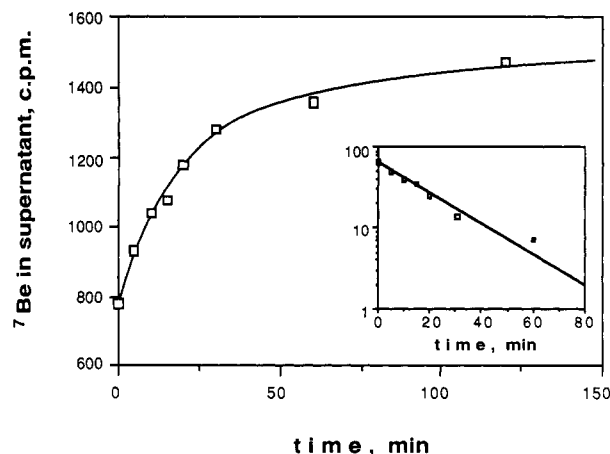
---

[2] Details of the mathematics used for derivation of eq 1 will be provided to the interested reader by writing directly to the authors.

FIGURE 3: Kinetics of BeF_3^- dissociation from microtubules. Tubulin was polymerized at 46 μM and was incubated with 10 μM ^{7}Be-labeled BeF_3^- for 90 min. A chase of 100 μM Be was then applied to the sample. Aliquots were rapidly sedimented in the airfuge at different time intervals following the chase. The amount of ^{7}Be in the supernatant was determined. The inset shows the semilogarithmic analysis of the data.
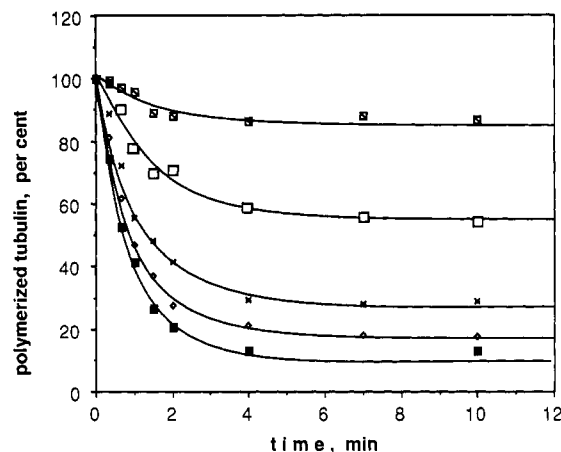

FIGURE 4: Microtubule depolymerization upon dilution in buffers containing different concentrations of BeF_3^-. Microtubules (30 μM tubulin) were polymerized to steady state in buffer A containing 0.5 mM GTP. At time zero, an aliquot of the microtubule solution was diluted 50-fold into polymerization buffer containing 2 mM NaF and the following concentrations of Be^{2+}: (solid box) 0 μM; (open diamond) 5 μM; (asterisk) 10 μM; (open box) 25 μM; (slashed box) 50 μM. The time course of depolymerization following dilution was monitored by using the glass filter assay (see Materials and Methods).

from microtubules within a first-order process $k_- = 6 \times 10^{-4}$ s^{-1}.

The combination of the values of the association and dissociation rate constants for the interaction of BeF_3^- with microtubule GDP subunits leads to an equilibrium dissociation constant $K = k_-/k_+ = 7 \pm 2$ μM, in reasonable agreement with equilibrium binding measurements. Table I summarizes the parameters for interaction of P_i and BeF_3^- with microtubules.

Correlation between the Extent of Binding of BeF_3^- to Microtubules and the Rate of Subunit Dissociation. The effect of BeF_3^- on the rate of microtubule depolymerization upon dilution was investigated by using the filter assay previously developed to study the stabilization of microtubules by inorganic phosphate. The following observations were made. (i) When microtubules were diluted in buffers containing different concentrations of BeF_3^-, the decrease in the rate of depolymerization linked to BeF_3 binding was not instantaneous but developed slowly during the depolymerization process, at a rate increasing in proportion with the concentration of BeF_3^- present in the dilution buffer. As a result,

the depolymerization curves, displayed in Figure 4, showed pseudo plateaus. This behavior is consistent with the slow binding of BeF_3^- to microtubules found above but contrasts with the immediate effect of P_i observed previously in the same assay. (ii) Microtubules preincubated for 1 h in the presence of BeF_3^- depolymerized at the same initial slow rate when diluted in buffers that did or did not contain BeF_3^- (data not shown). This observation is also consistent with the slow dissociation of BeF_3^- from microtubules. (iii) In further systematic experiments, microtubules (25 μM polymerized tubulin) were preincubated for 1 h at 37 °C in the presence of BeF_3^- at different concentrations in the range (0–100 μM) and then diluted in a buffer in the absence of BeF_3. The time courses of depolymerization upon dilution are shown in Figure 5a. The initial rate of depolymerization decreased apparently very cooperatively with the extent of BeF_3^- bound to microtubules, $\bar{Y}$. This peculiar behavior is only due to the fact that BeF_3^- dissociates very slowly from GDP subunits in microtubules. In other words, at the time of dilution, in the experiment of Figure 5a, $GDP–BeF_3$ tubulin subunits occupy defined positions in the microtubule. The time course of endwise depolymerization for a typical individual microtubule containing a few $GDP–BeF_3^-$ subunits is illustrated in Figure 5b and is shown to consist of a complex combination of rapid losses of GDP subunits ("catastrophe") intercalated with pauses due to the fact that $GDP–BeF_3$ subunits, when arriving at the tip of the microtubule in the course of the depolymerization, have a much longer lifetime $(1/k_-')$ than GDP subunits $(1/k_-)$. The complexity of this process is averaged out over a population of microtubules; the bulk population therefore will depolymerize at a rate k_-^{app} given by

$$\frac{1}{k_-^{app}} = \frac{\bar{Y}}{k_-'} + \frac{1 - \bar{Y}}{k_-}$$

which can be rearranged as

$$\frac{k_-}{k_-^{app}} = \bar{Y}(R - 1) + 1 \qquad (2)$$

where k_- is the rate of depolymerization of GDP–microtubules observed in the absence of BeF_3^- and $R = k_-/k_-'$. The value of $\bar{Y}$ can be calculated from the concentrations of total polymerized subunits T_0, total BeF_3^- concentration B_0, and equilibrium dissociation constant K according to

$$\bar{Y} = \frac{B_0 + T_0 + K \pm [(B_0 + T_0 + K)^2 - 4B_0T_0]^{1/2}}{2T_0} \qquad (3)$$

Note that (1) in deriving eq 2, we have assumed that no cooperative interactions take place between GDP and GDP–BeF_3 subunits and (2) according to eq 2, if, for example, $R = 10$, 10% of GDP–BeF_3 subunits in a microtubule ($\bar{Y} = 0.1$) will lead to a decrease as large as 2-fold in the rate of depolymerization.

The initial rates of depolymerization were measured by using the data in Figure 5a and plotted according to eq 2 in which $\bar{Y}$ was calculated from eq 3. Figure 5c shows that as long as $\bar{Y} < 0.5$, the data are adequately described by eq 3. A value of 23 $\pm$ 2 was derived for R, i.e., GDP–BeF_3^- subunits dissociate 23-fold more slowly from microtubule ends than GDP subunits. However, the plot curves upward above 50% saturation of microtubules by BeF_3^-, consistent with a cooperative increase in stability when at last one every other subunit has BeF_3^- bound. This piece of data indicates that the rate of dissociation of a terminal GDP–BeF_3^- subunit is cooperatively decreased when the adjacent subterminal subunit also carries BeF_3^-.
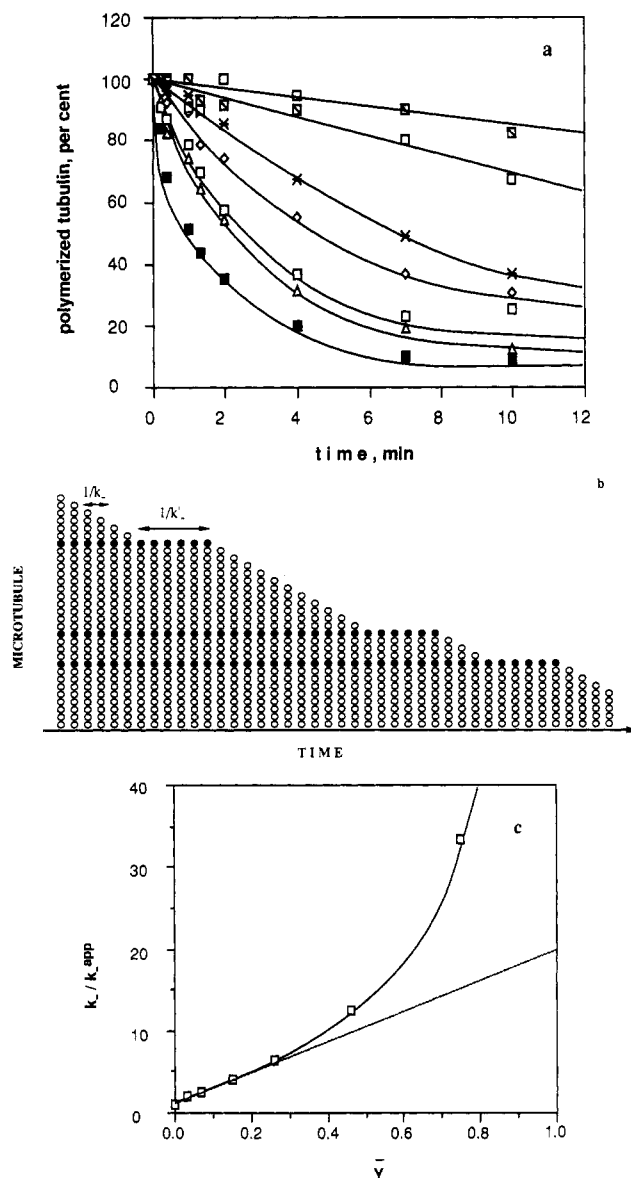

FIGURE 5: Correlation between the extent of BeF_3^- binding to microtubules and the stabilization of the polymer. (a) Time course of depolymerization upon dilution of microtubules preincubated in the presence of different concentrations of BeF_3^-. Microtubules (21 μM polymerized subunits) were polymerized for 60 min at 37 °C in the presence of 50 μM [^{3}H]GTP, 2 mM NaF, and the following concentrations of Be^{2+}: (solid box) 0 μM; (open triangle) 1 μM; (open box) 2.5 μM; (open diamond) 5 μM; (asterisk) 10 μM; (open box) 20 μM; (slashed box) 50 μM. At time zero, microtubules were diluted 50-fold in polymerization buffer containing no BeF_3^-. The time course of depolymerization was monitored by using the glass filter assay. (b) Schematic time course of endwise depolymerization of a microtubule containing a given proportion of GDP–BeF_3 subunits. A microtubule is schematized as a sequence of aligned circles representing tubulin subunits. Open circles represent GDP subunits and solid circles GDP–BeF_3 subunits. k_- and k_-' are the rate constants for dissociation of GDP and GDP–BeF_3 subunits, respectively, from microtubules ends. In the illustrated example, $k_-/k_-' = 6$; that is, a terminal GDP–BeF_3 subunit has a 6-fold longer lifetime at a microtubule end than a GDP subunit. (c) The reciprocal of the relative rate of depolymerization is plotted versus the extent of the BeF_3^- binding to microtubules, $\bar{Y}$, according to eq 2.

It should be pointed out that eq 2 applies only because BeF_3^- is not in rapid equilibrium with GDP subunits. Since BeF_3^- dissociates from GDP–tubulin at a much slower rate than GDP–BeF_3–tubulin from microtubule ends, a GDP–BeF_3 subunit can be considered in some way as a capping protein because it stays at the end for a long time. The same reasoning
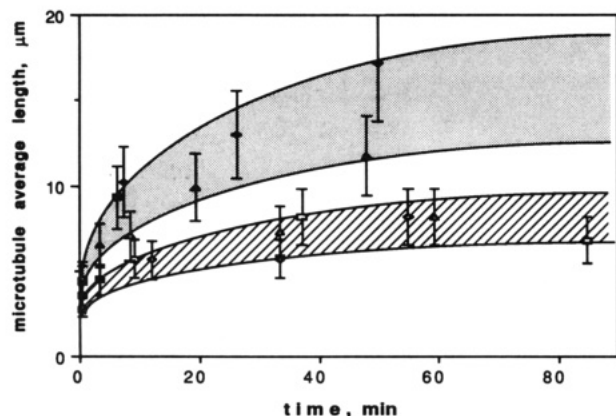
FIGURE 6: Effect of BeF$_3^-$ on the time course of redistribution in length of microtubules following shearing. Tubulin (40 μM) was polymerized and incubated at 37 °C for 30 min in the absence (solid symbols) or in the presence (open symbols) of 100 μM Be^{2+} and 2 mM NaF. At time zero, each solution was sheared. Histograms of distribution in length and determination of the average length were performed on each sample at different time intervals following the shear. The different symbols correspond to different series of experiments.

no longer applies to GDP–P$_i$ subunits because P$_i$ appears in rapid equilibrium with GDP subunits. In this case, the rate of depolymerization is

$$k^{app} = k_-'\bar{Y} + k_-(1 - \bar{Y}) \tag{4}$$

where $\bar{Y}$ is the probability that P$_i$ is bound to the terminal subunit and k_- and k_-' are the rate constants for GDP–tubulin and GDP–P$_i$–tubulin dissociation from microtubule ends, respectively. In previous experiments (Carlier et al., 1988a), the rate of depolymerization of microtubules has indeed been found to decrease linearly with the extent of P$_i$ bound according to eq 4.

Effect of BeF$_3^-$ on the Kinetics of Microtubule Redistribution in Length following Fragmentation. The molecular mechanism by which microtubules spontaneously undergo length redistribution following mechanical shear has been a subject of debate. Evidence has been shown for a true end-to-end reannealing process (Rothwell et al., 1986), while other works either observing the dynamics of individual microtubules (Kristofferson et al., 1986) or showing incorporation of [^{3}H]GTP into microtubules during the length redistribution process (Farrell et al., 1987) rather support a mechanism based on monomer–polymer reactions within which short polymers would disappear via endwise depolymerization into subunits that would in turn reassociate into longer polymers, via random walk processes as we have previously described for actin (Carlier et al., 1984b). In order to decide between these two mechanisms, microtubules polymerized in the presence or absence of 100 μM BeF$_3$ were sheared to an average length of 4 μm at time zero by two passages through a 26-gauge needle, and the kinetics of length changes following the shear were monitored by electron microscopy. Figure 6 shows that a 2.5-fold increase in length developed within 1 h in the absence of BeF$_3^-$, while the change in length was very small, during the same period of time, in the presence of BeF$_3^-$. Since the effect of BeF$_3^-$ is to reduce the rate of subunit dissociation, these observations provide support to the mechanism for length redistribution involving monomer–polymer exchange reactions. These findings are also in agreement with previous data showing inhibition of steady-state monomer–polymer exchange by BeF$_3^-$ (Carlier et al., 1988a).

Binding of BeF$_3^-$ to Dimeric and Oligomeric GDP–Tubulin. Equilibrium binding of ^{7}Be-labeled BeF$_3$ to GDP–tubulin was investigated by equilibrium dialysis either at low (0.25 mM)
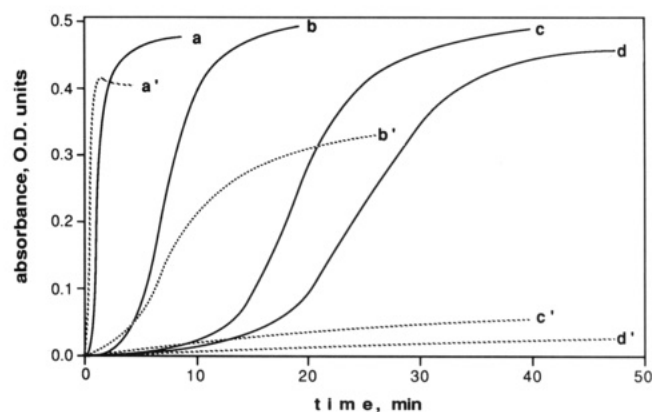

FIGURE 7: BeF$_3^-$ releases the inhibition of tubulin polymerization by GDP and promotes incorporation of GDP–tubulin into microtubules. The 1:1 GTP–tubulin complex (35 μM) was polymerized in the presence of GDP at the following concentrations: (a, a') 0 μM; (b, b') 100 μM; (c, c') 200 μM; (d, d') 300 μM. The assay also contained 200 μM Be^{2+} with (a–d) or without (a'–d') 5 mM NaF. Turbidity was recorded at 350 nm.

concentration of Mg^{2+}, where tubulin is essentially the $\alpha\beta$ dimer species, or at high (12 mM) Mg^{2+} concentration, where ring-shaped 40S oligomers are the predominant species (Howard & Timasheff, 1986). No binding was detected when tubulin concentration was as high as 55 μM; binding of BeF$_3^-$ with an equilibrium association constant as low as 5 × 10^3 M^{-1} could have been detected by this technique. Since the tubulin–tubulin interactions involved in GDP oligomers are of the same nature as the longitudinal interactions between tubulin subunits within the protofilaments of microtubules, we conclude that lateral interactions between tubulin subunits in the microtubule are necessary to BeF$_3^-$ binding.

Consistent with the above finding, no spontaneous polymerization of pure GDP–tubulin (70 μM) could be observed in the presence of BeF$_3^-$ at concentrations up to 200 μM, in agreement with a recent paper (Humphreys & MacDonald, 1988).

BeF$_3^-$ Releases the Inhibition of Microtubule Assembly by GDP and Promotes Incorporation of GDP–Tubulin into Microtubules. It is well established that GDP inhibits tubulin polymerization (Weisenberg et al., 1976; Carlier & Pantaloni, 1978). General agreement has been reached that only GTP–tubulin participates in microtubule assembly and GDP–tubulin is not incorporated into microtubules, except maybe under restrictive conditions (Hamel et al., 1986). However, GDP–tubulin appears able to block microtubule ends (Margolis, 1981; Zeeberg & Caplow, 1981; Engelborghs & Van Houtte, 1981; Carlier & Pantaloni, 1982; Carlier et al., 1988a), although a contrary view has been expressed (Martin & Bayley, 1987). In order to elucidate how the bound nucleotide affects the stability of tubulin–tubulin interactions in the microtubule, the following experiments have been carried out. GTP–tubulin 1:1 complex (30 μM) free of unbound GTP was incubated for 1–2 h at 0 °C in buffer A in the presence of different concentrations of GDP and 6 mM MgCl$_2$. The samples were then polymerized at 37 °C in the presence of 200 μM Be^{2+} and in either the presence or absence of 5 mM NaF.

Figure 7 shows that polymerization of GTP–tubulin was inhibited by GDP in the absence of BeF$_3^-$, as currently observed. This inhibition was greatly released by BeF$_3^-$: the lag time was shortened, and polymerization proceeded to the same extent as in the absence of GDP. Normal microtubules were observed in the electron microscope. In order to determine whether microtubules formed in the presence of GDP and BeF$_3^-$ were assembled from GTP subunits or from GDP

Table II: Effect of Inorganic Phosphate and Its Analogue BeF_3^- on the Rate Parameters for Tubulin Polymerization

	standard	$+P_i$	$+BeF_3^-$
elongation rate constant of GTP–tubulin (μM^{-1} s^{-1})	7	–	7
dissociation rate constant (GDP subunits) (s^{-1})	200	8	8[a]
elongation rate constant of GDP-tubulin (μM^{-1} s^{-1})	0	–	0.4

[a] This value represents the rate constant for dissociation of GDP–BeF_3 subunits below 50% saturation of the microtubule by BeF_3^-. As shown in Figure 5c, lower values are found above 50% saturation by BeF_3^-.

subunits, a similar experiment was carried out in which the [³H]GTP–tubulin 1:1 complex (30 μM) was polymerized in the presence of 250 μM GDP and 200 μM BeF_3^-. Microtubules were sedimented in the airfuge. The concentrations of dimeric tubulin and of ³H-labeled nucleotide in the supernatant were determined. The data (average of two experiments) show that 80–90% of the tubulin assembled in microtubules (22–24 μM) had unlabeled GDP as bound nucleotide. In contrast, in the control carried out in the absence of BeF_3, a very low amount of microtubules was formed, which were ³H-labeled in agreement with previous results (Carlier & Pantaloni, 1982). Therefore, in the presence of BeF_3^-, GDP–tubulin can be readily incorporated into microtubules. The conclusion of all the above experiments is that although dimeric GDP–tubulin does not bind BeF_3^- and is not able, in the presence of BeF_3^-, to undergo spontaneous polymerization into microtubules, its incorporation into microtubules that have been nucleated by a substoichiometric amount of GTP is made possible in the presence of BeF_3^-. In addition, at equilibrium, the amounts of microtubules formed either in the presence of GDP plus BeF_3^- or in the presence of GTP plus BeF_3^- were identical. Note that in the absence of fluoride, Be^{2+} and Al^{3+} did not bind to microtubules (Carlier et al., 1988a) and did not affect the polymerization of tubulin that is promoted here by Mg^{2+} ions.[3]

Kinetic Parameters for Elongation of Microtubules from GDP Subunits in the Presence of BeF_3^-. When microtubules are diluted isothermically in polymerization buffer, they depolymerize at a fast rate characteristic of GDP subunits endwise dissociation (Carlier et al., 1984). When the dilution buffer contains pure GDP subunits (in the total absence of GTP), GDP–tubulin is not able to support microtubule elongation but does bind to microtubule ends nonproductively (Caplow & Reid, 1985) and blocks depolymerization (Carlier et al., 1987a). GDP–tubulin therefore acts like a capping protein as functionally defined in the actin field (Korn, 1982; Craig & Pollard, 1982; Weeds, 1982). The experiments described in the preceding paragraph and showing that, in the presence of BeF_3^-, GDP–tubulin can be incorporated in microtubules, raise the need to analyze more quantitatively the mechanism and kinetic parameters for microtubule elongation

[3] Under the same conditions, i.e., when tubulin polymerization is promoted by millimolar amounts of Mg^{2+}, MacDonald and co-workers also did not observe any effect of Al^{3+} on tubulin polymerization and GTP hydrolysis [see curves f and g in Figure 4 of MacDonald et al. (1987)]. On the other hand, different results were obtained by these authors (MacDonald & Martin, 1988) when tubulin polymerization was promoted by low amounts of Al^{3+} in the absence of Mg^{2+} ions; in this case, some nonhydrolyzed GTP was found bound to microtubules and polymerization was inhibited by NaF, which—so do we presume—acted as a chelator of Al^{3+} and displaced it from tubulin, making it unable to polymerize. In contrast, we find that AlF_4^- binds as an analogue of P_i on microtubules assembled in the presence of Mg^{2+} ions.
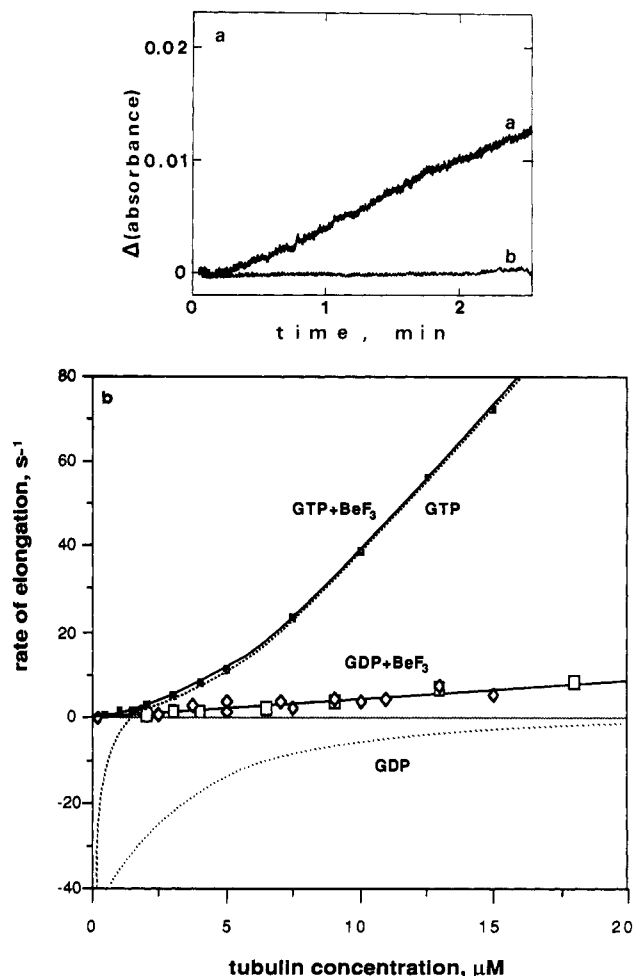

FIGURE 8: Effect of BeF_3^- on the rate of microtubule growth in the presence of GTP or GDP and its dependence on tubulin concentration. The initial rate of microtubule elongation was assayed turbidimetrically. The dimeric tubulin solution was equilibrated at 37 °C for 3 min in polymerization buffer containing 200 μM BeF_3^- before the seeds (1–2 μM polymerized tubulin coming from a 25 μM stock solution of assembled microtubules) were added to start the elongation process. The assay was carried out either in the presence of GTP–tubulin (solid symbols) or GDP–tubulin and 0.5 mM GDP (open symbols). In the latter case, 20 μM Ap_5A, 2 mM glucose, and 40 units/mL hexokinase were also included in the assay as previously described (Carlier et al., 1987a). Panel a represents the time course of turbidity change following the addition of seeds to 10 μM GDP–tubulin in the presence of 200 μM BeF_3^- (a). Curve b is the control in which no seeds were added to the solution of 10 μM GDP–tubulin in the presence of 200 μM BeF_3^-. Panel b represents the rates of elongation from GTP or GDP subunits in the presence of BeF_3, as indicated. Identical data were obtained whether the seed solution also contained (◇) or did not contain (□) 200 μM BeF_3^-. Dashed curves represent the control curves obtained in the absence of BeF_3^- (Carlier et al., 1987a) both in the presence of GTP or in the presence of GDP as indicated.

from GDP subunits in the presence of BeF_3^-. Figure 8 shows that in the presence of 200 μM BeF_3^- elongation of microtubules was supported by GDP–tubulin. Practically the same rate, within 20%, was observed in the presence of a 2.5-fold larger amount of BeF_3^-. The rate of elongation J increased linearly with the concentration c of GDP–tubulin in the range investigated (0–18 μM). The straight line extrapolated to a value of the critical concentration ($J = 0$) very close to zero. A value of 0.43 μM^{-1} s^{-1} was derived from the slope of the $J(c)$ plot for the association rate constant of GDP–tubulin to microtubule ends in the presence of BeF_3^-. This value is 16-fold lower than that found here at 37 °C (6.95 μM^{-1} s^{-1}) for association of GTP subunits in a regime of rapid growth
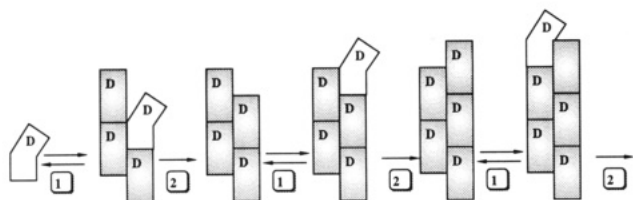
FIGURE 9: Schematic representation of microtubule elongation from exogenous GDP subunits in the presence of BeF$_3^-$. GDP–tubulin dimer is featured with a bent shape (Carlier et al., 1987a). GDP–BeF$_3$ subunits in microtubules are shadowed. The elongation process takes place in two steps: Step 1 is nonproductive binding of GDP–tubulin to an elongating site. The subsequent step 2 is binding of BeF$_3^-$ to the terminal GDP subunit with an associated isomerization into the microtubular conformation of the GDP–BeF$_3$ subunit. Steps 1 and 2 repeated lead to effective elongation.

(Carlier et al., 1987a). The effect of BeF$_3^-$ on the rate of elongation of GTP subunits was also investigated. In a regime of net growth, at $c > 2$ μM, the rate of elongation was not affected by BeF$_3^-$; in contrast, below the critical concentration, BeF$_3^-$ slowed down the rate of dissociation of GDP subunits from microtubules (Carlier et al., 1988a) and thus prevented the catastrophic depolymerization of the GDP core observed in the absence of BeF$_3^-$ (Carlier et al., 1984a). Consequently, the $J(c)$ plot in the presence of GTP plus BeF$_3^-$ extrapolated, at $J = 0$, to the same low value of the critical concentration as the $J(c)$ plot in the presence of GDP plus BeF$_3^-$, and the steep downward curvature below the critical concentration was abolished. The rate parameters for microtubule elongation in the absence or presence of BeF$_3^-$ are displayed in Table II.

The elongation of microtubule seeds from GDP–tubulin in the presence of BeF$_3^-$ can be explained as follows: when microtubules are diluted to a final concentration of 2 μM GDP subunits into polymerization buffer containing 200 μM BeF$_3^-$, within 5 s following dilution the amount of GDP–BeF$_3$ subunits formed will be equal to $k_+(\text{TGDP})_{\text{MT}} \times \text{BeF}_3 \times 5$ s, i.e., 100 $\times 10^{-6} \times 2 \times 200 \times 5 = 0.2$ μM, that is 1 every 10 subunits in the microtubule. The time course of depolymerization of the GDP–microtubule induced by dilution will be blocked as soon as a GDP–BeF$_3$ subunit reaches the terminal position of the microtubule (Figure 5b). A few seconds later, more extensive binding of BeF$_3^-$ ensures a high stability of the seed, as documented in Figure 4. If the buffer in which microtubules are diluted also contains GDP–tubulin, which has been shown to bind to microtubule ends with an equilibrium constant of 4–6 μM (Carlier et al., 1987a), the equilibrium association of a GDP–tubulin to an end followed by BeF$_3^-$ binding will result in the effective incorporation of this exogenous GDP subunit as a new microtubule subunit. The same process repeated on and on leads to elongation of microtubules from GDP–tubulin followed by stabilization by BeF$_3^-$. Eventually a low critical concentration is achieved in the presence of GDP and BeF$_3^-$, as can be observed in Figures 7 and 8. The simple scheme drawn in Figure 9 describes the proposed mechanism and accounts for the data.

The fact that, in a regime of net growth, the rate of microtubule elongation from GTP–tubulin is unaffected by BeF$_3^-$ demonstrates that terminal subunits are not GDP subunits and dissociate at a slow rate consistent with the rate of dissociation of GDP–BeF$_3$ subunits. Since we have shown (Carlier et al., 1987a) that in a regime of slow growth the rate of cleavage of the γ-phosphate of GTP is identical with the rate of microtubule elongation and no appreciable GTP cap can be detected, the simplest comprehensive interpretation of all data thus far is that in a regime of slow growth and at steady state GDP–P$_i$ subunits are present at the growing ends of micro-

tubules, where they form a stabilizing cap due to their slow dissociation rate. The size of this GDP–P$_i$ cap should depend on the combination of the rates of association of GTP–tubulin, cleavage of GTP (40 s^{-1} at 30 °C), release of P$_i$, and dissociation of GDP–P$_i$ subunits.

DISCUSSION

The interaction of BeF$_3^-$, a structural analogue of inorganic phosphate, with GDP–tubulin subunits of microtubules and its effect on the kinetics of microtubule assembly have provided clues to the involvement of GTP hydrolysis in microtubule dynamics. The main conclusions we reach are the following.

BeF$_3^-$ associates to and dissociates from microtubule GDP subunits at slow rates ($k_+ \simeq 90$–100 M^{-1} s^{-1}; $k_- = 6 \times 10^{-4}$ s^{-1}) as compared to the natural substrate P$_i$ and also binds with a 3 orders of magnitude higher affinity than P$_i$ (Carlier et al., 1988a). These results suggest a binding mechanism involving a rapid equilibrium, low-affinity binding followed by a slow conformation change leading to a large increase in the affinity of BeF$_3^-$; the dissociation of BeF$_3^-$ would be kinetically limited by the slow reversal ($k = 6 \times 10^{-4}$ s^{-1}) of this conformation change. Such binding characteristics are typical of analogues of the transient state in enzyme catalysis, as defined by Lienhard et al. (1971), and applied to the phosphoryl-transfer reaction of ribonuclease (Lindquist et al., 1973). Orthovanadate, another analogue of inorganic phosphate, also interacts slowly and with a higher affinity than P$_i$ with ribonuclease and a number of other enzymes involved in phosphohydrolase and phosphotransferase reactions, including myosin (Goodno, 1979). Phosphate, vanadate, and (BeF$_3^-$, H$_2$O) are all three tetrahedral in solution; however, the present results suggest that BeF$_3^-$ might find the proper nucleophilic environment, in the GTP site, to adopt the trigonal bipyramidal pentacoordinate structure characteristic of the transition state (Dennis & Westheimer, 1966; Lienhard et al., 1971).

Although BeF$_3^-$ exhibits simple Michaelian binding to microtubules, interestingly, the fact that BeF$_3^-$ is not in rapid equilibrium with GDP–tubulin leads to an apparent cooperative increase in stability with the degree of BeF$_3^-$ binding to microtubules: only 1 GDP–BeF$_3^-$ subunit every 20 GDP subunits in the microtubule will cause a 50% decrease in the rate of depolymerization of the population. In the course of the depolymerization process, when a GDP–BeF$_3$–tubulin subunit arrives at the tip of the microtubule, it remains there for a 20-fold longer time than a GDP subunit and temporarily blocks further depolymerization. Incidentally, the above behavior may also have some physiological relevance with regard to tubulin microheterogeneity in the cell: if a tubulin subspecies dissociates from microtubules at a slower rate than others, either because P$_i$ is released extremely slowly following GTP hydrolysis or for any other conformational reason, then only a few percent enrichment of some microtubules in this particular tubulin may give them an extensive specific stability. These microtubules are expected to represent a poorly dynamic population in the cell, because of the high probability of the presence of a slowly dissociating tubulin subspecies at their ends at steady state. The time course of depolymerization of an individual microtubule containing a small percentage of stabilizing subspecies will also exhibit a complex sequence of rapid shortenings and pauses as illustrated in Figure 5b.

It is interesting to note that BeF$_3^-$ does not bind to dimeric nor oligomeric (rings) GDP–tubulin. BeF$_3^-$ therefore binds only to a polymeric structure in which tubulin hydrolyzes GTP. This observation supports the view that BeF$_3^-$ binds to the catalytic GTPase site of tubulin and that the conformation of the nucleotide site is different whether tubulin possesses (in

microtubules) or does not possess (in the $\alpha\beta$ dimer or in the ring) a GTPase activity. BeF_3^- therefore is expected to be an interesting tool in the tridimensional study of the nucleotide site and of its conformation change in the course of the catalysis.

Use of BeF_3^-, as mimicking the GDP-P_i state of microtubule, has been helpful to understand the involvement of the elementary steps of GTP hydrolysis in tubulin polymerization, in particular, how the bound nucleotide affects tubulin–tubulin interactions. Three main conclusions can be derived from the effect of BeF_3^- on the tubulin concentration dependence of the rate of microtubule elongation [$J(c)$ plot, Figure 8b]. First, the coincidence of the two curves obtained without BeF_3^- above the critical concentration in the presence of GTP confirms our proposal (Carlier et al., 1988a) that in a regime of slow growth and at steady state terminal GDP-P_i subunits, structurally and functionally similar to GDP-BeF_3 subunits, form a stabilizing cap that prevents the depolymerization of the GDP core. Second, the steep deviation from linearity of the $J(c)$ function at the critical concentration, which is the basis for microtubule dynamic instability, is abolished when microtubules remain in the intermediate GDP-P_i state; in other words, P_i release following cleavage of GTP is the regulatory switch that is responsible for the nonlinearity of $J(c)$ in GTP and triggers the dynamic instability behavior of microtubules. This view is consistent with the higher stability of microtubules polymerized in the presence of poorly hydrolyzable Cr-GTP (MacNeal & Purich, 1978; Gaskin, 1981) and GTPβS(B) (Roychowdhury & Gaskin, 1988). Whether GDP-P_i–tubulin is energetically similar to GTP–tubulin in the polymerized state depends on the extent of reversibility of GTP hydrolysis. As a comparison, note that ATP hydrolysis associated to actin polymerization has been found essentially irreversible (Carlier et al., 1988b). Third, BeF_3^- allows incorporation of GDP-tubulin in microtubules. The data (Figures 7 and 8) can be accounted for by the following interpretation: GDP–tubulin blocks microtubule ends with an equilibrium dissociation constant of 4 μM (Carlier et al., 1987a). BeF_3^- binding induces a conformation change of this GDP subunit, allowing tighter tubulin–tubulin interactions in microtubules and hence sequential incorporation of exogenous GDP–tubulin in the lattice.

The nature of the tubulin–tubulin interaction in microtubule that is regulated by P_i release following cleavage of GTP and undergoes a switch from "strong" in the GDP-P_i state to "loose" in the GDP state is an important issue. The longitudinal interaction between tubulin subunits in protofilaments is unlikely to depend on GTP hydrolysis because, as mentioned above, BeF_3^- does not bind with high affinity to ring oligomers which presumably directly derive from protofilaments (Kirschner et al., 1974; Erickson, 1974). The strength of lateral interactions is therefore more likely to be regulated by P_i release; however, the details of the conformational switch must await further work.

Finally, the role of nucleotide hydrolysis and more especially of P_i release following cleavage of the γ-phosphate is of general significance in the dynamics of the two major components of the cytoskeleton, i.e., actin filaments and microtubules. In the case of actin, too, P_i release following ATP hydrolysis is associated with the destabilization of the filament (Carlier & Pantaloni, 1988); AlF_4^- and BeF_3^- also bind tightly, within a slow equilibrium, to F-ADP-actin subunits in the site of the γ-phosphate of ATP and mimic the effects of P_i on F-actin dynamics (Carlier & Combeau, 1988).

Registry No. GTP, 86-01-1.

REFERENCES

Bigay, J., Deterre, P., Pfister, C., & Chabre, M. (1985) *FEBS Lett. 191*, 181–185.

Caplow, M., & Reid, R. (1985) *Proc. Natl. Acad. Sci. U.S.A. 82*, 3267–3271.

Carlier, M.-F. (1982) *Mol. Cell. Biochem. 47*, 97–110.

Carlier, M.-F., & Pantaloni, D. (1978) *Biochemistry 17*, 1908–1915.

Carlier, M.-F., & Pantaloni, D. (1981) *Biochemistry 20*, 1918–1924.

Carlier, M.-F., & Pantaloni, D. (1982) *Biochemistry 21*, 1215–1224.

Carlier, M.-F., & Pantaloni, D. (1988) *J. Biol. Chem. 263*, 817–825.

Carlier, M.-F., & Combeau, C. (1988) *J. Biol. Chem.* (in press).

Carlier, M.-F., Hill, T. L., & Chen, Y. (1984a) *Proc. Natl. Acad. Sci. U.S.A. 81*, 771–775.

Carlier, M.-F., Pantaloni, D., & Korn, E. D. (1984b) *J. Biol. Chem. 259*, 9987–9991.

Carlier, M.-F., Didry, D., & Pantaloni, D. (1987a) *Biochemistry 26*, 4428–4437.

Carlier, M.-F., Melki, R., Pantaloni, D., Hill, T. L., & Chen, Y. (1987b) *Proc. Natl. Acad. Sci. U.S.A. 84*, 5257–5261.

Carlier, M.-F., Didry, D., Melki, R., Chabre, M., & Pantaloni, D. (1988a) *Biochemistry 27*, 3555–3559.

Carlier, M.-F., Pantaloni, D., Evans, J. A., Lambooy, P. K., Korn, E. D., & Webb, M. R. (1988b) *FEBS Lett. 235*, 211–214.

Craig, S. W., & Pollard, T. D. (1982) *Trends Biochem. Sci. 7*, 88–92.

Dennis, E. A., & Westheimer, F. H. (1966) *J. Am. Chem. Soc. 88*, 3431–3432.

Engelborghs, Y., & Van Houtte, A. (1981) *Biophys. Chem. 14*, 195–202.

Erickson, H. P. (1974) *J. Cell Biol. 60*, 153–167.

Farrell, K. W., Jordan, M. A., Miller, H. P., & Wilson, L. (1987) *J. Cell Biol. 104*, 1035–1046.

Gaskin, F. (1981) *Biochemistry 20*, 1318–1322.

Goodno, C. C. (1979) *Proc. Natl. Acad. Sci. U.S.A. 76*, 2620–2624.

Hamel, E., Batra, J. K., & Lin, C. M. (1986) *Biochemistry 25*, 7054–7062.

Hill, T. L., & Carlier, M.-F. (1983) *Proc. Natl. Acad. Sci. U.S.A. 80*, 7234–7238.

Horio, T., & Hotani, H. (1986) *Nature (London) 321*, 605–607.

Howard, W. D., & Tismasheff, S. N. (1986) *Biochemistry 25*, 8292–8300.

Humphreys, W. G., & MacDonald, T. L. (1988) *Biochem. Biophys. Res. Commun. 151*, 1025–1032.

Job, D., Pabion, M., & Margolis, R. L. (1985) *J. Cell Biol. 101*, 1680–1689.

Kirschner, M. W., Williams, R. C., Weingarten, M., & Gerhart, J. C. (1974) *Proc. Natl. Acad. Sci. U.S.A. 71*, 1159–1163.

Korn, E. D. (1982) *Physiol. Rev. 62*, 672–737.

Korn, E. D., Carlier, M.-F., & Pantaloni, D. (1987) *Science 238*, 638–644.

Kristofferson, D., Mitchison, T., & Kirschner, M. (1986) *J. Cell Biol. 102*, 1007–1019.

Lange, A. J., Arion, W. J., Burchell, A., & Burchell, B. (1986) *J. Biol. Chem. 261*, 101–107.

Lienhard, G. E., Secemski, I. I., Koehler, K. A., & Lindquist, R. N. (1971) *Cold Spring Harbor Symp. Quant. Biol. 36*, 45-51.

Lindquist, R. N., Lynn, J. L., Jr., & Lienhard, G. E. (1973) *J. Am. Chem. Soc. 95*, 8762-8768.

MacDonald, T. L., & Martin, R. B. (1988) *Trends Biochem. Sci. 13*, 15-19.

MacDonald, T. L., Humphreys, W. G., & Martin, R. B. (1987) *Science 236*, 183-188.

MacNeal, R. L., & Purich, D. L. (1978) *Arch. Biochem. Biophys. 191*, 233-243.

Margolis, R. L. (1981) *Proc. Natl. Acad. Sci. U.S.A. 78*, 1586-1590.

Martin, S. R., & Bayley, P. M. (1987) *Biophys. Chem. 27*, 67-76.

Mitchison, T., & Kirschner, M. (1984) *Nature 312*, 237-242.

Rothwell, S. W., Grasser, W. A., & Murphy, D. B. (1986) *J. Cell Biol. 102*, 619-627.

Roychowdhury, S., & Gaskin, F. (1988) *Biochemistry 27*, 7799-7805.

Shelanski, M. L., Gaskin, F., & Cantor, C. R. (1973) *Proc. Natl. Acad. Sci. U.S.A. 70*, 765-768.

Weeds, A. (1982) *Nature 296*, 811-815.

Weingarten, M. D., Lockwood, A. H., Hwo, S. Y., & Kirschner, M. W. (1975) *Proc. Natl. Acad. Sci. U.S.A. 72*, 1858-1862.

Weisenberg, R. D., Deery, W. J., & Dickinson, P. J. (1976) *Biochemistry 15*, 4248-4254.

Zeeberg, B., & Caplow, M. (1981) *J. Biol. Chem. 256*, 12051-12057.

Kinetics of Interleukin 2 mRNA and Protein Produced in the Human T-Cell Line Jurkat and Effect of Cyclosporin A

René Nordmann,[*,‡] Elsebeth Andersen,[‡] René Trussardi,[‡] and Norman A. Mazer[§,‖]

Departments of Preclinical Research and Pharmaceutical Product Development, Pharmaceutical Division, Sandoz Ltd., CH-4002 Basle, Switzerland

ABSTRACT: The kinetics of interleukin 2 mRNA accumulation in the leukemic T-cell line Jurkat, which can be induced with phytohemagglutinin and phorbol 12-myristate 13-acetate to produce large amounts of interleukin 2, was analyzed by a modified DNA-excess solution hybridization assay using a $5'$-^{32}P-labeled oligodeoxyribonucleotide 30 bases long as probe. Cyclosporin A was used as a valuable tool to gain more insight into the quantitative aspects of interleukin 2 production, on the basis of the assumption that transcription of the interleukin 2 gene is completely inhibited shortly after administration of cyclosporin A. The half-life of interleukin 2 mRNA was estimated to be approximately 2 h. With the aid of simple mathematical models, we have been able to relate the concentration of interleukin 2 protein in the supernatant to the interleukin 2 mRNA kinetics. This novel quantitative kinetic analysis revealed that, independent of the absence or presence of cyclosporin A, interleukin 2 protein is synthesized at a rate of approximately 1.3 molecules per molecule of interleukin 2 mRNA per second and secreted within 2 h after it is synthesized and that its half-life in the supernatant is approximately 10 h.

Interleukin 2 (IL2),[1] or T-cell growth factor, has been recognized as a key immunoregulatory protein for the proliferation of activated T-cells of various types. Studies of the control of IL2 expression in T-cells have revealed that IL2 production is induced at the transcriptional level upon antigenic or mitogenic stimulation. Moreover, it has been shown that cyclosporin A (Sandimmune, CsA), a powerful immunosuppressive drug of considerable clinical importance, inhibits the expression of the IL2 gene (Arya & Gallo, 1987; Kaempfer et al., 1987; Paetkau et al., 1987).

In order to gain more insight into the quantitative aspects of IL2 production, we have studied the kinetics of IL2 mRNA and secreted IL2 protein produced in the human T-cell line Jurkat and the influence of CsA added at different times after induction. To assay IL2 mRNA, we have modified existing solution hybridization methodology and developed a versatile

method using a chemically synthesized $5'$-^{32}P-labeled oligodeoxyribonucleotide as single-stranded probe. In vitro synthesized IL2 mRNA served as a hybridization standard and was also used to evaluate the sensitivity of the assay. By a novel approach, applying simple mathematical models, we have been able to estimate from our kinetic data the absolute rates of IL2 mRNA production and IL2 protein synthesis, as well as the half-lives of both species. The general applicability of using our assay method and models for studying the kinetics of other mRNA species is discussed, and criteria for choosing suitable oligonucleotide probes by computer analysis of mRNA sequences are offered.

MATERIALS AND METHODS

Stimulation of Jurkat Cells and Determination of IL2 Protein in the Supernatant. Jurkat leukemic T cells (subclone K16) were grown in RPMI 1640, containing 10% fetal calf serum, 2 mM L-glutamine, 100 units/mL penicillin, 100

---
[*] Address correspondence to this author.
[‡] Department of Preclinical Research.
[§] Department of Pharmaceutical Product Development.
[‖] Present address: TheraTech, Inc., Research Park, 410 Chipeta Way, Suite 219, Salt Lake City, UT 84108.

---
[1] Abbreviations: CsA, cyclosporin A; HLA-B, major histocompatibility antigen B; IL2, interleukin 2; PHA, phytohemagglutinin; PMA, phorbol 12-myristate 13-acetate; AUC, area under the curve.